Title of Grant / Cooperative Agreement:	GLOBAL ASSESSMENT OF STRATIFORM BOUNDARY LAYER CLOUDS FROM AQUA: REDUCING UNCERTAINTIES IN THE MAGNITUDE OF THE FIRST INDIRECT AEROSOL EFFECT
Type of Report:	Summary of Research
Name of Principal Investigator:	Ralf Bennartz
Period Covered by Report:	Jan 2009 - Jan 2012
Name and Address of recipient's institution:	Space Science & Engineering Center University of Wisconsin 1225 W. Dayton St. Madison, WI, 53713
NASA Grant / Cooperative Agreement Number:	NNX08AF92G

Reference 14 CFR § 1260.28 Patent Rights *(abbreviated below)*
The Recipient shall include a list of any Subject Inventions required to be disclosed during the preceding year in the performance report, technical report, or renewal proposal. A complete list (or a negative statement) for the entire award period shall be included in the summary of research.

Subject inventions include any new process, machine, manufacture, or composition of matter, including software, and improvements to, or new applications of, existing processes, machines, manufactures, and compositions of matter, including software.

Have any Subject Inventions / New Technology Items resulted from work performed under this Grant / Cooperative Agreement?	[x] NO	[ ] YES
If yes a complete listing should be provided here: Details can be provided in the body of the Summary of Research report.		

1) Project overview

The following three goals are to be addressed in the project: (1) The combination of MODIS, AMSR-E, and CERES on Aqua allow to experimentally quantify the variability of cloud droplet number concentration and cloud geometrical thickness as well as their impact on shortwave albedo. Cloud droplet number concentration is of high scientific relevance by itself, but it also establishes a global reference dataset for validation of global climate models (GCMs). (2) Regional studies of variability of cloud droplet number concentration were performed. These studies allow studying the impact of e.g. biomass burning events on cloud albedo. Those studies make use of auxiliary information such as backwards trajectories to link changes in cloud microphysics to regional sources. Changes in cloud droplet number concentration to anthropogenic sources based on aerosol observations and transport models. Each step will be accompanied by an extensive error analysis of all components within the process leading to realistic error estimates for all derived parameters. The results of these findings are documented in the peer-reviewed literature listed below.

2) Peer reviewed publication fully or partly supported by this project

1. **Bennartz, R., A. Lauer, J.-L. Brenguier, 2011**: Scale-aware integral constraints on autoconversion and accretion in regional and global climate models. Geophys. Res. Lett., 38, L10809, doi:10.1029/2011GL047618.
2. **Bennartz, R., J. Fan, J. Rausch, R. Leung, A. Heidinger, 2011**: Pollution from China increases cloud droplet number, suppresses rain over the East China Sea. Geophys. Res. Lett., 38, L09704, doi:10.1029/2011GL047235.
3. **Bennartz, R., P. Watts, J. F. Meirink, and R. Roebeling, 2010**: Rain water path in warm clouds derived from combined visible/near-infrared and microwave satellite observation. *J. Geophys. Res.* doi:10.1029/2009JD013679.
4. **Foster, M. J., R. Bennartz, and A. K. Heidinger, 2011**: Estimation of Warm Cloud Properties that Conserve Total-scene Reflectance Using Near-infrared Satellite Measurements, *Journal of Applied Meteorology and Climatology*, 50, 1,96-109.
5. **Hoose, C., U. Lohmann, R. Bennartz, B. Croft, and G. Lesins, 2008**: Global simulations of aerosol processing in clouds, Atmos. Chem. Phys., 8, 6939-6963.
6. **Lauer, A., K. Hamilton, Y. Wang, V. Phillips, R. Bennartz, 2010:** The impact of global warming on marine boundary layer clouds over the eastern Pacific – A regional model study, Journal of Climate, 23, 5844-5863
7. **Lauer, A., Y. Wang, V. T. J. Phillips, C. S. McNaughton, R. Bennartz, and A. D. Clarke, 2009:** Simulating marine boundary layer clouds over the eastern Pacific in a regional climate model with double-moment cloud microphysics, J. Geophys. Res., 114, D21205, doi:10.1029/2009JD012201.
8. **Makkonen, R., Asmi, A., Korhonen, H., Kokkola, H., Järvenoja, S., Räisänen, P., Lehtinen, K. E. J., Laaksonen, A., Kerminen, V.-M., Järvinen, H., Lohmann, U., Bennartz, R., Feichter, J., and Kulmala, M., 2009**: Sensitivity of aerosol concentrations and cloud properties to nucleation and secondary organic distribution in ECHAM5-HAM global circulation model, Atmos. Chem. Phys., 9, 1747-1766.
9. **Menon, S., A. D. Del Genio, Y. Kaufman, R. Bennartz, D. Koch, N. Loeb, and D. Orlikowski**, **2008**: Analyzing signatures of aerosol-cloud interactions from satellite retrievals and the GISS GCM to constrain the aerosol indirect effect. Journal of Geophysical Research, 113, doi: 10.1029/2007JD009442.
10. **Qian, Y., D. Gong, J. Fan, L. R. Leung, R. Bennartz, D. Chen, and W. Wang, 2009**: Heavy pollution suppresses light rain in China: Observations and modelling. J. Geophys. Research, doi:10.1029/2008JD011575.
11. . **Rausch, J., A. Heidinger, and R. Bennartz, 2010**: Regional assessment of marine boundary layer cloud microphysical properties using the PATMOS-x data. J. Geophys. Res., doi:10.1029/2010JD014468.
12. **Storelvmo, T., U. Lohmann, and R. Bennartz, 2009**: What governs the spread in shortwave forcings in the transient IPCC AR4 models?, *Geophys. Res. Lett.*, *36*, L01806, doi:10.1029/2008GL036069.
13. **Wood, R., M. Koehler, R. Bennartz, and C. W. O'Dell, 2009**: The diurnal cycle of divergence over the global oceans. Quarterly Journal of the Royal Meteorological Society. Part B, Vol. 135, 1484-1493.

3) Master's and Ph.D. thesis

Two M.S. thesis resulted under partial support of this project. John Rausch finished his M.S. at the Department of Atmospheric and Oceanic Sciences, University of Wisconsin – Madison in spring 2009. The thesis title is: "Global Assessment of the Microphysical Properties of Marine Boundary Layer Clouds Using a Long-Term Satellite Climatology". John is staying on for a Ph.D. also under partial support of this project. Na-Young Kim finished her M.S. degree in fall 2011.

4) Selected Science results

Chinese SO_2 emissions have increased by more than a factor of three over the last 30 years. Here we show that these changes significantly affect wintertime clouds and precipitation over the East China Sea downwind of major emission sources. Satellite observations show an increase of cloud droplet number concentration from less than 200 cm^{-3} in the 1980s to more than 300 cm^{-3} in 2005. In the same time period, precipitation frequency reported by voluntary ship observers was reduced from more than 30% to less than 20% of the time. A back trajectory analysis showed the pollution in the investigation area to originate from the Shanghai-Nanjing and Jinan industrial areas. A model sensitivity study was performed, isolating the effects of changes in SO_2 emissions on clouds and precipitation using a state-of-the-art mesocale model including chemistry and aerosol indirect effects. Similar changes in cloud droplet number concentration over the East China Sea were obtained when the current industrial emissions in China were reduced to the 1980s. Simulated changes in precipitation were somewhat smaller than the observed changes but still significant.

Increased air pollution levels in China and downwind have received great attention over the last decades. The effects of air pollution on solar radiation budget at the surface are quite significant and straightforward to observe[1]. The impact of rising pollution levels on clouds and precipitation is equally important but much harder to assess[2,3]. Lumped together in the term 'aerosol indirect effects' various suggested mechanisms of aerosol-cloud-precipitation interactions constitute the largest uncertainties in current estimates of global anthropogenic climate forcing[4]. Previous studies linking aerosols with clouds and precipitation were often focusing on subtropical stratocumulus cloud regimes off the west coast of the continents. Changes in those stratocumulus regimes have important climatic implications. However, those cloud systems do not produce much precipitation, and cover only small fractions of the globe. Other studies have inferred the potential influence of aerosols on precipitation in other climate regimes[5,6], but quantitative relationships between changes in clouds and precipitation and aerosol source regions have not yet been firmly established[2].

Here we study the impact of pollution on clouds and precipitation up to more than 1000 km downwind of the sources of pollution over the East China Sea. During winter cold high passages occur over China approximately once every 4 days. As the high pressure moves to the East China Sea, it undergoes a significant transformation due to the strong sensible and latent heat fluxes from the warm ocean surface. Active cumulus convection develops and clouds form in the moist and unstable stratification above the sea surface[7]. Rapid cyclogenesis can also occur in the baroclinic zone as cold air moves over the warm East China Sea and the Kuroshio Current, leading to explosive cyclogenesis and large amounts of precipitation[8]. How aerosols affect cloud and precipitation in these varied cloud regimes is not clear. We evaluate a 30-year time series of observations of liquid cloud properties and precipitation. Satellite observations allow for an estimation of cloud droplet number concentration (CDNC)[9,10], a key variable in determining the impact of pollution on cloud microphysics. Precipitation frequency is studied based on voluntary ship observer reports[11]. The strong correlative evidence of indirect aerosol effects found in the observational datasets is substantiated with a modeling study substantiating a causal relation between changes in air pollution and subsequent changes in clouds and precipitation.

Observed changes in cloud droplet number concentration and precipitation

Figure 1 shows the wintertime cloud droplet number concentration (CDNC) derived from Patmos-X satellite observations. Between 1982 and 2009 CDNC in the investigation area have increased in the investigation area with an

average rate of increase of +42 cm^{-3}/10yrs (linear regression slope). Values in the early 1980s are in the order of 200 cm^{-3} while in the late 2000s values are in excess of 300 cm^{-3}. These trends are statistically significant at the 99%+ level (Two-sided Student's t-test) and also clearly exceed what can be attributed to satellite drifts and inter-calibration issues[12]. Are the trends observed in CDNC correlated with trends in precipitation? If so, is the increase in CDNC causing changes in precipitation? Arguments can be made for both questions to be answered in the affirmative. [6] have made a case for pollution suppressing light rain over China. The combined modeling and observational analysis performed in their paper suggested that indeed elevated CDNC values caused by pollution inhibit collision-coalescence processes in warm rain. Using TRMM observations and observed aerosol distributions [13] show that elevated aerosol concentrations might lead to reduced collision-coalescence over the East China Sea as well. Addressing the issue from a cloud microphysical standpoint, various observational and modeling studies use combinations of cloud droplet number concentration and liquid water path to establish drizzle rates for stratocumulus cloud fields[10,14-17]. These studies find roughly an inverse relation between CDNC and light rain (drizzle) rate. Extending this *1/*CDNC-scaling argument to our case one would predict a decrease in warm rain by roughly 30% (relative) between 1980 and 2010, inversely proportional to an increase in CDNC from 200 cm^{-3} around 1980 to 300 cm^{-3} around 2010 (see Figure 1). This back-of-the-envelope calculation would suggest a decrease in precipitation dominated by warm cloud processes.

Actual precipitation trends are difficult to assess, especially over the oceans, where conventional data are sparse. Satellite-based precipitation estimates are not an option. Existing passive microwave climatologies, e.g. from Special Sensor Microwave/Imager (SSM/I), are not suitable for cloud-aerosol interaction studies because of technical issues associated with the separation of rain from cloud liquid water. By design this separation eliminates potential sensitivities[13,18,19]. Space-borne radar observations do not yet provide long enough coverage (CloudSat) or are insensitive to light rain (TRMM-PR). While trends in precipitation intensity cannot be assessed reliably, some information about precipitation frequency is available from weather observations made by voluntary ship observers provided via the International Comprehensive Ocean-Atmosphere Dataset (ICOADS)[11].

Based on ICOADS, Figure 2 shows precipitation frequency plots for the years 1982-1986 and 2004-2009. Large differences between the earlier and later years are seen in a latitude belt between roughly 15 N and 40 N. The average rain frequency in the investigation area is reduced from about 30% (absolute) for 1982 -1986 to about 20% (absolute) for 2004-2009, or by about 40% relative to the long-term mean value. A negative trend is apparent in all three precipitation classes (Table 1). In order to eliminate spurious trends we performed a series of tests, the results of which are summarized in Table 1. In particular, we address the following three issues: (1) Are the trends statistically significant? We performed two-sided Student t-tests for all trends. We find the trends in all three precipitation classes to be statistically significant at the 99% confidence level. Obviously, this statistical significance by itself does not allow for any conclusion on the physical significance of the trend, i.e. it does not answer the question whether the trend in observations is caused by a trend in actual precipitation. (2) Might the trends then be caused by outliers toward the beginning or the end of the time series? As noted earlier, the ICOADS time series is only quality controlled until 2007. Also, from Figure 2 it is apparent that for the years 1982-1985 precipitation frequency appears to be exceptionally high. We therefore re-calculated the trends for the years 1986 – 2007 only. The resulting trends for the intermediate and low rain classes were similar to those found for the entire period. The trends in light and intermediate rain remain high at -16.7%/10yrs and -17.4 %/10yrs and at confidence levels of higher than 99%. Only the trend in heavy precipitation is reduced significantly and the confidence level drops to 66%. (3) Could the trends perhaps be introduced by changes in observer habits, reporting differences, or postprocessing of the ICOADS data? Changes in observer routine have been reported in earlier studies[20]. If trends were caused by such changes, we would expect the trends to appear in a similar manner globally. To test this hypothesis, we selected a reference area in the South Pacific where large changes in aerosol load are not to be expected and CDNC is virtually constant over time[12]. For the South Pacific reference area we do not find any statistically significant negative trend although an apparent positive trend in intermediate rain is found for the shorter time interval (1986-2007). As a result of these tests we might cautiously conclude that the large trends in

light and intermediate precipitation in winter over the China Sea are possibly physical. Given there are no similar trends identified in the reference area systematic changes caused by observer habits and/or changes in data processing do not appear to be causing the trends in precipitation.

Obviously, there are various possible candidate physical explanations including the cloud-aerosol interaction hypothesis, but possibly also correlations with changes in the Asian Monsoon, or changes in large-scale circulation patterns. In wintertime, the atmospheric flow over China and the East China Sea is dominated by a very stable high pressure system over northern Asia inducing a strong near-zonal continental outflow in the middle atmosphere and a northwesterly boundary layer wind. This flow pattern provides an effective mechanism for transporting pollution originating in the large industrial areas onto the East China Sea. We use a back-trajectory model[21] in combination with a SO_2 emission inventory[22] to determine the source regions of pollution reaching the investigation area. To further disentangle the effects of local pollution from changes in e.g. large-scale circulation patterns and other possible sources of trends, we have performed a modeling sensitivity study using WRF-Chem.

Airmass origin and source regions

Back trajectory origins and SO2 source regions are given in Figure 3. For each back trajectory, the uptake is calculated as the product of SO_2 emission from the REAS database multiplied by uptake efficiency (function of height for each back trajectory) and then summed over all back trajectories that originate in the grid box. The Shanghai-Nanjing and Jinan industrial areas can be clearly identified as hot spots for emissions transported into the investigation area within 48 hours. Figure 3c shows time series of all-China SO_2 emissions, back-trajectory SO_2 uptake for the investigation area at 48 hours lead-time, ICOADS rain frequency and 1/CDNC. All four curves are normalized to zero mean and unit standard deviation. In addition the SO_2 emissions and uptake are multiplied by -1 in order to compare slopes and variability to the other two datasets. Correlation between Chinese SO_2 emissions and 1/CDNC (rain frequency) is 0.83 (0.80). Correlations for SO_2 uptake for individual back-trajectories lead times peaked at 48 hours with values of 0.72 (0.70) for 1/CDNC (rain frequency). Correlation between rain frequency and 1/CDNC is 0.85. All correlations were found to be significant at the 99.9 % or higher level.

Modeling results

The observational results presented here suggest a strong impact of Chinese SO_2 emissions on cloud properties and precipitation frequency over the East China Sea. In a modeling study using a state-of-the-art mesoscale meteorological and chemical model, WRF-Chem, we investigated the causality of the relation between changes in mainland China SO_2 emissions and changes in downwind cloud and precipitation properties by isolating the impact of SO_2. A two month simulation using WRF-Chem was performed with current day emissions ('POLLUTED' run, see online supplement) and emissions scaled back to the 1980s ('CLEAN' run, see online supplement). Everything else, in particular the meteorological conditions, remained unchanged between the two runs. In good agreement with the observations the average CDNC increased from 208 cm^{-3} to 295 cm^{-3} between the CLEAN and POLLUTED case. A reduction in precipitation frequency from CLEAN to POLLUTED is simulated as well but less pronounced than the observed decreases in precipitation frequency. The absolute precipitation frequency in the model is about twice as high as in the observations: 44% (CLEAN) and 39% (POLLUTED), which is typical of coarse scale atmospheric simulations. The absolute reduction in precipitation of 5% between the CLEAN and POLLUTED experiments is about half of the observed change. The resulting relative changes (Table 1) show a decrease in the order of one third of the observations. There might be various reasons for the differences between observed and simulated precipitation response, including the aforementioned uncertainties in the observational datasets, unaccounted changes in precipitation response to factors other than CDNC (e.g. changes in sea surface temperature and atmospheric circulation), shortcomings in the model's representation of precipitation in general, and in the model's representation of aerosol effects on precipitation in particular.

Implications.

The long-term observations studied here imply a strong impact of pollution from China on clouds and precipitation over large parts of the East China Sea, which possibly also affects adjacent countries such as Japan, Taiwan, and Korea. With the more widespread use of filter technology in energy generation the observed effects would be expected to become weaker in subsequent years. Continuing satellite observations will allow monitoring of these changes. Marked by a convectively mixed layer and frequent cyclogenesis producing clouds and precipitation, the East China Sea might serve as a natural testbed, in contrast to the more extensively studied stratocumulus regimes, for assessing the ability of global climate models to reproduce aerosol indirect effects, which constitute a major uncertainty in our current understanding of anthropogenic climate forcing. The observed response of the clouds and precipitation to changes in pollution might also help assess the validity and potential environmental consequences of geoengineering approaches that alter cloud albedo by providing additional cloud condensation nuclei to reduce surface warming.

Datasets and Methods

Satellite Observations: This study uses NOAA Pathfinder Atmospheres – Extended (PATMOS-x) Level 2b cloud products, which are on a 0.2 x 0.2 degree equal-area grid. PATMOS-x is an Advanced Very High Resolution Radiometer (AVHRR) data product that provides daily surface and atmospheric climate records from 1981 to the present[23]. The AVHRR is a multi-channel visible and infrared imaging radiometer deployed aboard several National Oceanic and Atmospheric Administration (NOAA) polar orbiting environmental satellites (POES) since 1979. The AVHRR does not provide onboard calibration sources for the 0.63, 0.86 and 1.6 mm channels. The calibration methodology employed in PATMOS-x is described in [24]. Cloud droplet number concentration (CDNC) of marine boundary layer clouds are inferred from PATMOS-x Level 2b retrievals of optical thickness and cloud droplet effective radius using the method of [10]. A novel approach to addressing artifacts in CDNC due to satellite orbital drift is applied by normalizing estimated droplet number concentrations with respect to local observation time. The details of the this method as well as a detailed discussion of remaining uncertainties and potential artifacts in the data are given in [12].

Precipitation observations: The International Comprehensive Ocean-Atmosphere Dataset (ICOADS) [11] provides an archive of various marine surface observations over the global oceans. The current version (2.5) is available from UCAR's data archive (DS 540.0) and provides quality controlled and homogenized data from 1662 until 2007. Data beyond 2007 are available as well but as of now did not undergo extensive quality control or homogenization. For the present study we are interested in the frequency of occurrence of precipitation and use present weather observations provided by voluntary ship observers. Our methodology follows the work of [20] (hereafter termed 'P95') who used a predecessor dataset to evaluate the frequency of precipitation over the global oceans. P95 also addresses various caveats and potential pitfalls associated with the subjective nature of the visual classifications and potential inhomogeneities in the dataset. The potential bearing of these caveats on the current study is discussed further in the results section. Similar to P95 we classify different types of precipitation based on the present weather codes. Different from P95 we concentrate on liquid precipitation only, excluding all frozen or partially frozen precipitation classes. Another slight modification from P95 is that we only distinguish three classes of precipitation intensity: light, intermediate, and heavy precipitation. We neglect other dimensions (e.g. intermittent versus continuous) and focus more on the lighter precipitation. These changes appear prudent since we are dealing with extratropical precipitation and are only interested in frequency of occurrence. In the online supplement we provide the exact mapping between present weather code and the precipitation intensity classes used.

Back-trajectories and SO_2 emission database: For estimating the origin of air masses the Hybrid Single-Particle Lagrangian Inegrated Trajectory model (HYSPLIT4[21]) provided by NOAA's Air Resource Laboratory was used. Back trajectories were calculated using National Center for Environmental Prediction (NCEP) reanalysis meteorological fields. Back trajectories were calculated for the entire study period and region (every 5 degrees and every third day) starting at 500 m (i.e. within the boundary layer) leading to about 200 back trajectories each individual month and about 18000 for each season (200 x 30 years x 3 months). Calculations were performed backward in time for 72 hours. Every 12 hours the height and position of the back trajectory were evaluated. Using the entire back trajectory dataset density, maps of airmass origin for different 12-hourly time lags were generated. In addition to the airmass origin

statistics a simple SO_2 uptake was modeled based additionally on the parcel's height at a given lag time and SO2 emissions based on the Regional Emission Inventory in Asia (REAS[22]), which provides annually averaged SO_2 emissions for the south east Asian area at 0.5 degrees spatial resolution between 1980 and 2009. For each back trajectory an uptake efficiency was modeled as a simple exponential function with a scale height of 1500 m, i.e., if the uptake efficiency is unity at the surface, it is reduced to *1/e* at 1500 meters. For each 1x1 degree grid-box the total SO_2 uptake was then modeled as the efficiency times the REAS SO_2 emission value.

Mesocale model: We employ WRF-Chem with the updated two-moment Lin microphysical scheme in which droplet number concentrations are predicted [25], to perform regional scale simulations to support our hypothetical reasons for the observed results. The WRF-Chem model is configured with the RADM2 (Regional Acid Deposition Model 2) photochemical mechanism [26] and the MADE/SORGAM (Modal Aerosol Dynamics Model for Europe (MADE) and Secondary Organic Aerosol Model (SORGAM)) aerosol model [27,28]. Meteorological fields are assimilated using lateral boundary and initial conditions from NCEP/NCAR Global reanalysis data. Chemical lateral boundary conditions are from the default profiles in WRF-Chem. Anthropogenic emissions are obtained from the Reanalysis of the TROpospheric (RETRO) chemical composition inventories (http://retro.enes.org/index.shtml). Biomass burning emissions are obtained from the Global Fire Emissions Database, Version 2 (GFEDv2.1) with 8-day temporal resolution [29]. We conduct a base run referred to as POLLUTED for the winter season from Dec. 25, 2004 to Feb. 15, 2005 with the current emissions. We scaled the gas-phase emissions of SO_2 and NO_x and the primary aerosol emissions of sulfate, nitrate, and $PM_{2.5}$, and PM_{10} by a factor of 0.3 over land and conducted a sensitivity run referred to as CLEAN for comparison. Simulations were run on a domain comprised of 160×110 grid points with a 36 km horizontal resolution that covers most of China and part of the West Pacific Ocean.

Tables and Figures

Table 1: Trends observed in wintertime ICOADS ship observations for light, intermediate, and heavy rain over the East China Sea (18-34N, 120-132.5E) and over a reference area in the South Pacific (10-60S, 90-180W). Trends were calculated for the winter months of 1982 - 2009 and 1986 – 2007. All trends are given in percent per decade. Significance levels of trends (SIG) were calculated using a two-sided Student t-test and are given in percent. Trends with a statistical significance larger than 95% are highlighted bold. Corresponding WRF-Chem results for precipitation frequency and intensity are also shown.

		1982-2009		1986-2007		WRF-Chem	WRF-Chem
		Frequency [%/10yrs][#]	SIG	Frequency [%/10yrs][#]	SIG	Frequency [%/10yrs] [*]	Intensity [%/10yrs][+]
China	Light	**-13.4**	**99**	**-16.7**	**99**	-5.0	-5.0
	Intermediate	**-16.6**	**99**	**-17.4**	**99**	-2.1	-1.7
	Heavy	**-8.0**	**99**	-5.3	66	-5.2	-5.8
Pacific	Light	+1.5	49	+2.4	53	**N/A**	**N/A**
	Intermediate	+6.8	93	**+13.8**	**99**	**N/A**	**N/A**
	Heavy	-3.8	34	+0.6	4	**N/A**	**N/A**

[#]: The observational estimates are the regression slopes for precipitation frequency as a function of year. Relative percentages for the observations are derived as $100 \cdot \frac{s}{f_{1982}}$ where *s* is the regression slope and f_{1982} is the precipitation frequency in 1982. Values are expressed in [%/10yrs]

[*]: The WRF-Chem estimates were derived as $100 \cdot \frac{f_{Poll} - f_{Clean}}{2.5 \cdot f_{Poll}}$, where f_{Poll} and f_{Clean} are the rain frequencies for the polluted and clean cases, respectively. In order to make model and observation values comparable, the division by 2.5 normalizes the model changes to roughly [%/10yrs] by accounting for the fact that the polluted scenario compares emissions from 2005 (f_{Poll}) with emissions scaled by a factor of 0.3, which correspond roughly to 1980 (f_{Clean}), i.e. 2.5 decades earlier. WRF-Chem intensity classes were defined based on surface rain rate as 'light': 0.01— 0.1 mm/h; 'intermediate': 0.1— 5 mm/h; 'heavy': > 5 mm/h.

[+]: Intensity estimates were calculated the same way as frequency estimates but with rain rates instead of occurrence. Intensity estimates are only available from WRF-Chem but not from the observations.

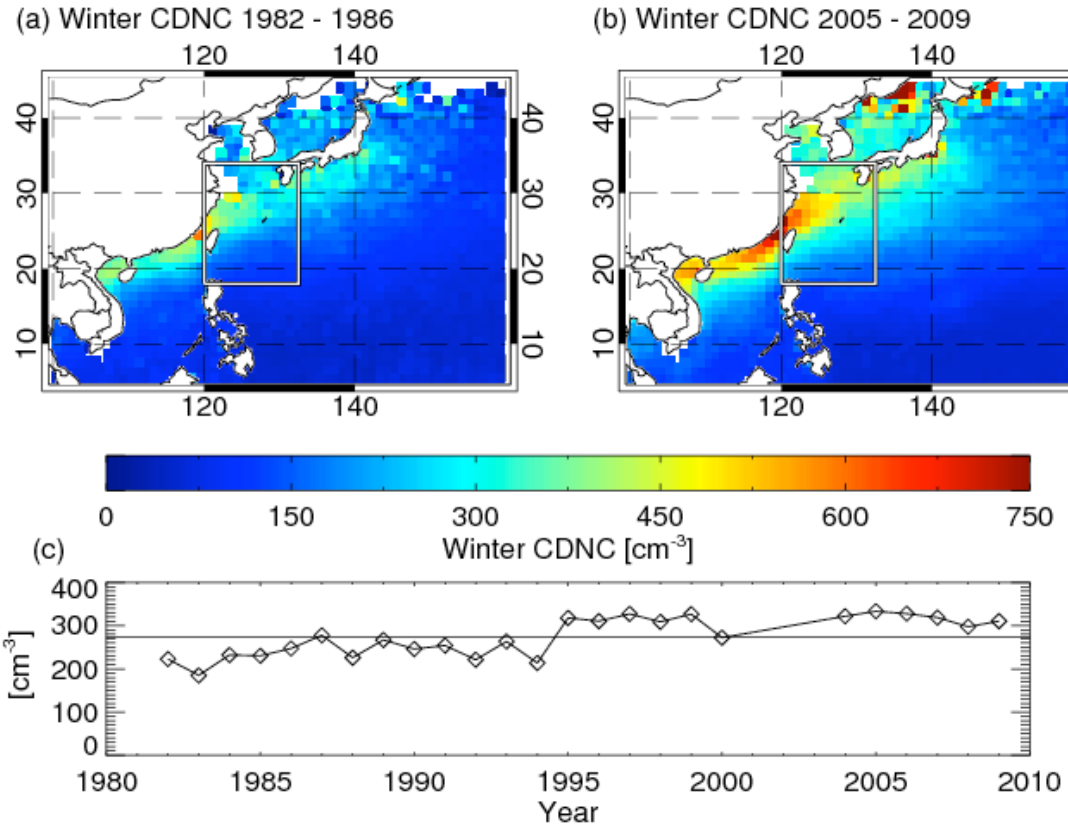

Figure 1: Panel (a) shows the PATMOS-x derived CDNC averaged over five winter seasons (1982-1986). Panel (b) shows the same for the winter seasons 2004-2009. The rectangular box in panels (a) and (b) highlights the investigation area. Panel (c) shows monthly mean CDNC averaged over the investigation area for December, January, and February 1982 – 2009. The black solid line in panel (c) corresponds to the long-term mean value.

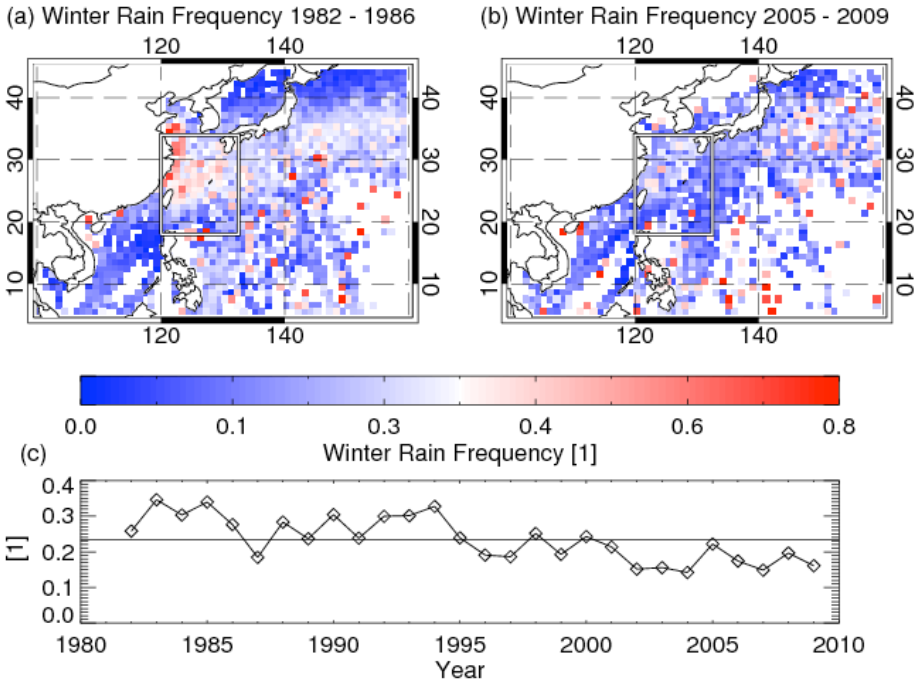

Figure 2: Frequency of occurrence of rainfall as reported by ICOADS voluntary ship observers. Panels (a) and (b) show the frequency of occurrence of all liquid rain events reported by ship observers for the winters 1982-1986 and 2004-2009, respectively. Panel (c) shows the time series of winter liquid rain frequency. For individual statistics separated by intensity, see Table 1. The black line in panel (c) represents the long-term mean rain frequency.

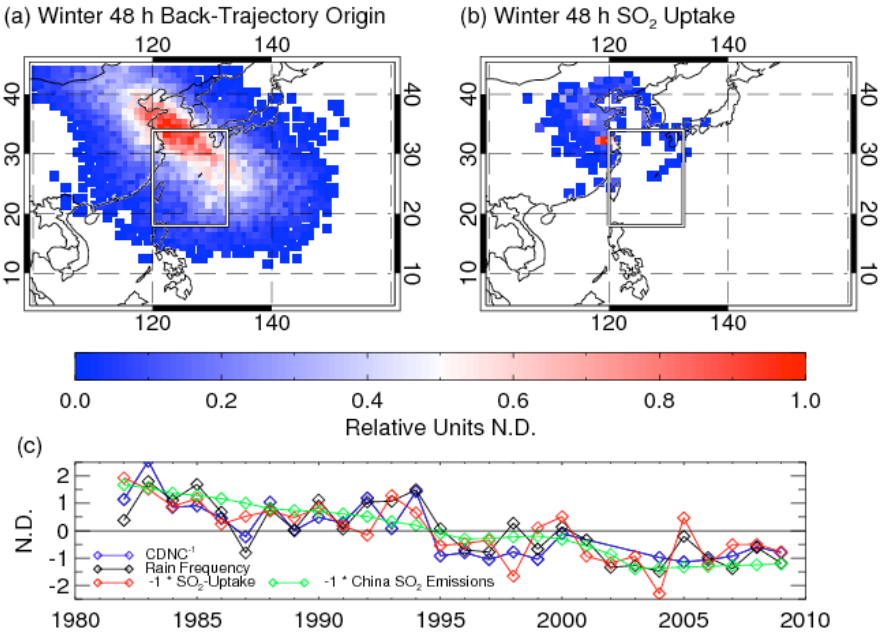

Figure 3: Panel (a) shows the relative density of origins of back-trajectories that end in the investigation area after 48 hours. Panel (b) shows the SO_2 uptake derived from 48 h back-trajectory origins and the SO_2 emission database. Values in panels (a) and (b) are normalized to a peak value of one. Panel (c) compares the total China SO_2 emissions (green curve), the 48 h SO_2 uptake (red curve) with rain frequency (black curve, same as in Figure 1c) and $CDNC^{-1}$ (blue curve). All values in panel (c) are normalized to zero mean and unit standard deviation. For visualization purposes the SO_2 uptake (red curve) and total China emission (green curve) are multiplied by -1.

References

1 Nakajima, T. *et al.* Significance of direct and indirect radiative forcings of aerosols in the East China Sea region. *Journal of Geophysical Research-Atmospheres* **108**, doi:8658 10.1029/2002jd003261 (2003).

2 Stevens, B. & Feingold, G. Untangling aerosol effects on clouds and precipitation in a buffered system. *Nature* **461**, 607-613, doi:10.1038/nature08281 (2009).

3 Rosenfeld, D. *et al.* Flood or drought: How do aerosols affect precipitation? *Science* **321**, 1309-1313, doi:10.1126/science.1160606 (2008).

4 Forster, P., Ramaswamy, P., Artaxo, P. & al., e. *Changes in Atmospheric Constituents and Radiative Forcing*. (Cambridge University Press, Cambridge, United Kingdom and New York, NY, USA., 2007).

5 Rosenfeld, D. & Givati, A. Evidence of orographic precipitation suppression by air pollution-induced aerosols in the western United States. *Journal of Applied Meteorology and Climatology* **45**, 893-911 (2006).

6 Qian, Y. *et al.* Heavy pollution suppresses light rain in China: Observations and modeling. *J Geophys Res-Atmos* **114**, doi:D00k02 10.1029/2008jd011575 (2009).

7 Ding, Y. H. & Krishnamurti, T. N. Heat budget of Siberian high and the winter monsoon. *Mon. Wea. Rev.* **115**, 2428-2449 (1987).

8 Hanson, H. P. & Long, B. Climatology of cyclogenesis over the East China Sea. *Mon. Wea. Rev.* **113**, 697-707 (1985).

9 Brenguier, J. L. *et al.* Radiative properties of boundary layer clouds: Droplet effective radius versus number concentration. *Journal of the Atmospheric Sciences* **57**, 803-821 (2000).

10 Bennartz, R. Global assessment of marine boundary layer cloud droplet number concentration from satellite. *J Geophys Res-Atmos* **112**, doi:doi:10.1029/2006JD007547 (2007).

11 Kent, E. C., Woodruff, S. D. & Berry, D. I. WMO Publication No. 47 metadata and an assessment of observation heights in ICOADS. *J. Atmos. Oceanic Technol.* **24**, 214-234 (2007).

12 Rausch, J., Heidinger, A. K. & Bennartz, R. Regional assessment of marine boundary layer cloud microphysical properties using the PATMOS-x dataset. *J. Geophys. Res.* **in press.**, doi:10.1029/2010JD014468 (2010).

13 Berg, W., L'Ecuyer, T. & Kummerow, C. Rainfall Climate Regimes: The Relationship of Regional TRMM Rainfall Biases to the Environment *Journal of Applied Meteorolgy and Climatology* **45**, 434-454 (2006).

14 Pawlowska, H. & Brenguier, J. L. An observational study of drizzle formation in stratocumulus clouds for general circulation model (GCM) parameterizations. *Journal of Geophysical Research-Atmospheres* **108**, 8630-8630 (2003).

15 vanZanten, M. C., Stevens, B., Vali, G. & Lenschow, D. H. Observations of drizzle in nocturnal marine stratocumulus. *Journal of the Atmospheric Sciences* **62**, 88-106 (2005).

16 Geoffroy, O., Brenguier, J. L. & Sandu, I. Relationship between drizzle rate, liquid water path and droplet concentration at the scale of a stratocumulus cloud system. *Atmospheric Chemistry and Physics* **8**, 4641-4654 (2008).

17 Comstock, K. K., Wood, R., Yuter, S. E. & Bretherton, C. S. Reflectivity and rain rate in and below drizzling stratocumulus. *Quarterly Journal of the Royal Meteorological Society* **130**, 2891-2918, doi:10.1256/qj.03.187 (2004).

18 Seethala, C. & Horvath, A. Global Assessment of AMSR-E and MODIS Cloud Liquid Water Path Retrievals in Warm Oceanic Clouds. *J. Geophys. Res.*, doi:doi:10.1029/2009JD012662 (2010).

19 O'Dell, C. W., Wentz, F. J. & Bennartz, R. Cloud liquid water path from satellite-based passive microwave observations: A new climatology over the global oceans. *Journal of Climate* **21**, 1721-1739 (2008).

20 Petty, G. W. Frequencies and Characteristics of Global Oceanic Precipitation from Shipboard Present-Weather Reports. *Bulletin of the American Meteorological Society* **76**, 1593-1616 (1995).

21 Draxler, R. R. HYSPLIT4 user's guide. . *NOAA Tech. Memo. ERL ARL-230, NOAA Air Resources Laboratory, Silver Spring, MD.* (1999).

22 Ohara, T. *et al.* An Asian emission inventory of anthropogenic emission sources for the period 1980–2020. *Atmos. Chem. Phys. Discuss.* **7**, 4419-4444, doi:doi:10.5194/acp-7-4419-2007 (2007).

23 Thomas, S., Heidinger, A. K. & Pavolonis, M. Comparison of NOAA's Operational AVHRR-Derived Cloud Amount to Other Satellite-Derived Cloud Climatologies. *J. Climate* **17**, 4805-4822 (2004).

24 Heidinger, A. K., Straka III, W. C., Molling, C. C., Sullivan, J. T. & Wu, X. Deriving an Inter-sensor Consistent Calibration for the AVHRR Solar Reflectance Data Record. *International Journal of Remote Sensing* **in press.** (2010).

25 Chapman, E. G. *et al.* Coupling aerosol-cloud-radiative processes in the WRF-Chem model: Investigating the radiative impact of elevated point sources. . *Atmos. Chem. Phys.* **9**, 945–964 (2009).

26 Stockwell, W. R., Middleton, P., Chang, J. S. & Tang, X. The second generation regional acid deposition model chemical mechanism for regional air quality modeling. *J. Geophys. Res.* **95**, 16343–16367 (1990).

27 Ackermann, I. J. *et al.* Modal aerosol dynamics model for Europe: Development and first applications. *Atmos. Environ.* **32**, 2981–2999 (1998).

28 Schell, B., Ackermann, I. J., Hass, H., Binkowski, F. S. & Ebel, A. Modeling the formation of secondary organic aerosol within a comprehensive air quality modeling system. *J. Geophys. Res.* **106**, 28275–28293 (2001).

29 Randerson, J. T., R., V. d. W. G., Giglio, L., Collatz, G. J. & Kasibhatla, P. S. Global Fire Emissions Database, Version 2 (GFEDv2. 1). Available at http://daac.ornl.gov/ from Oak Ridge National Laboratory Distributed Active Archive Center, Oak Ridge, Tennesse, USA. doi:doi 10.3334/ORNLDAAC/849 (2005).